Chinese Journal of Aeronautics, (2017), xxx(xx): xxx–xxx

Chinese Society of Aeronautics and Astronautics
& Beihang University

Chinese Journal of Aeronautics

cja@buaa.edu.cn
www.sciencedirect.com

Multi-EAP: Extended EAP for multi-estimate extraction for SMC-PHD filter

Li Tiancheng [a,*], **Juan M. Corchado** [a], **Sun Shudong** [b], **Fan Hongqi** [c]

[a] *School of Science, University of Salamanca, Calle Espejo s/n, 37008 Salamanca, Spain*
[b] *School of Mechanical Engineering, Northwestern Polytechnical University, 710072 Xi'an, China*
[c] *ATR Key Laboratory, National University of Defense Technology, 410073 Changsha, China*

Received 1 March 2016; revised 15 April 2016; accepted 16 May 2016

KEYWORDS

Data association;
EAP estimator;
Multi-target tracking;
PHD filter;
Particle filter

Abstract The ability to extract state-estimates for each target of a multi-target posterior, referred to as multi-estimate extraction (MEE), is an essential requirement for a multi-target filter, whose key performance assessments are based on accuracy, computational efficiency and reliability. The probability hypothesis density (PHD) filter, implemented by the sequential Monte Carlo approach, affords a computationally efficient solution to general multi-target filtering for a time-varying number of targets, but leaves no clue for optimal MEE. In this paper, new data association techniques are proposed to distinguish real measurements of targets from clutter, as well as to associate particles with measurements. The MEE problem is then formulated as a family of parallel single-estimate extraction problems, facilitating the use of the classic expected a posteriori (EAP) estimator, namely the multi-EAP (MEAP) estimator. The resulting MEAP estimator is free of iterative clustering computation, computes quickly and yields accurate and reliable estimates. Typical simulation scenarios are employed to demonstrate the superiority of the MEAP estimator over existing methods in terms of faster processing speed and better estimation accuracy.

1. Introduction

Multi-target filtering (MTF) is concerned with the detection and state-estimation of a time-varying and unknown number of moving targets based on a sequence of noisy sensor measurements that are corrupted by clutter and misdetections. Given that the final filter outcome is provided in the form of individual tracks for each target, it is often referred to as multi-target tracking (MTT) for which extracting estimates for each target from the multi-target posterior lies at the core. MTF/MTT has a long history of research, over 50 years, with many applications in both military and commercial realms, including air traffic control, surveillance, aerospace, oceanography, autonomous vehicles and robots, remote sensing, and bioinformatics research.[1] Cutting edge overviews of MTT and popular state-of-the-art MTT algorithms can be found in Refs.[2,3].

* Corresponding author.
E-mail address: t.c.li@usal.es (T. Li).
Peer review under responsibility of Editorial Committee of CJA.

ELSEVIER Production and hosting by Elsevier

http://dx.doi.org/10.1016/j.cja.2016.12.025

Please cite this article in press as: Li T et al. Multi-EAP: Extended EAP for multi-estimate extraction for SMC-PHD filter, *Chin J Aeronaut* (2017), http://dx.doi.org/10.1016/j.cja.2016.12.025

Apart from handling the uncertainty in the state space model, one has to account for many more challenges arising in realistic environments. These include target detection (namely determining the number of targets that is time-varying), false alarms due to clutter, misdetections and, most challengingly, data association, which involves determining which target generated which measurement, if any. At the core of them, data association is strongly coupled with target detection, false alarms and misdetections and its implementation distinguishes two main groups of multi-target filters/trackers. On the one hand, traditional "divide and conquer" approaches treated the MTT problem as a number of separate single-target tracking problems based on the measurement-to-track (M2T) association, each of which is resolved using a suitable filter. As the key to these solutions, the "divide" operation refers to the M2T association and is executed prior to filtering. Consequently, multi-estimate extraction (MEE), as an essential task for displaying tracks, is straightforward, and each estimate is conditionally independent of the others.

On the other hand, targets and measurements can be naturally modeled by the use of random finite sets (RFS), which do not need to consider data order. By doing so, the problem of multiple target filtering in the presence of clutter and misdetection can be cast in a Bayesian framework,[4] resulting in an optimal multi-target Bayesian filter without performing M2T association. Instead of propagating the multi-target posterior density, the probability hypothesis density (PHD) filter[5] propagates the PHD, which is the first-order statistical moment of the RFS of multi-target states (which is also the intensity of the multi-target evolving point process). This affords a concise yet adequate RFS solution to MTF problems, which gains Kullback-Leibler divergence (KLD) minimization to approximate the posterior distribution,[6,7] and has recently elicited considerable attention. To note, there are also some other RFS multi-target filters driven based on different prior assumptions, e.g. the multi-Bernoulli prior results in a multi-Bernoulli filter,[4,8] which are beyond the scope of this paper.

Compared to the M2T association based MTF solutions, the advantage of the PHD filter is that it needs neither to associate measurements to tracks nor to distinguish real measurements of targets from the clutter at the filtering stage. However, this causes a challenge for MEE in the sequential Monte Carlo (SMC)-PHD implementation for nonlinear systems where the particles are basically not labelled to tracks and are indistinguishable. This is a serious problem simply because a tracker working with a bad MEE solution cannot be good, no matter how good the posterior obtained is. "Labelled" random finite sets[9] that integrate the track label into the state for estimating can partially avoid this MEE difficulty; however, this is much more algorithmically and computationally complicated and is beyond the scope of this paper. In addition, Ref.[10] further argues that "attempting to perform track formation using labelled filtering posterior densities departs from this ideal in two ways. First, using filtering posterior densities effectively treats as the object of interest the individual target states, collected in a vector or a set, at a particular time. This is at odds with the actual aim of estimating sequences of states. Second, in order to compensate for the lack of trajectory information in the filtering densities, labels which have no physical significance are added to the state." For one reason or another, we limit ourselves to the RFS filters without labelling.

The preconceived and possibly the most widely used MEE solution for the SMC-PHD filter is based on cluster analysis of the particle distribution, the essence of which is the particle-to-track association. Various clustering methods have been tailored in this respect, such as expectation-maximization algorithm,[11] k-means clustering,[11,12] fuzzy c-means and soft clustering,[13] finite mixture models,[14] CLEAN,[15,16] ant clustering[17] and some others proposed in Refs.[18–20]. However, most of them lack strong theoretical justifications.[21]

Clustering is generally an iterative computing process that often suffers from problems of non-convergence, unreliability and slow computing speed. When the estimated number of targets does not match the natural number of clusters, the clustering output, which is naturally not scalable with the number of targets, is likely to be significantly erroneous.[6] In contrast, measurement-oriented methods that are free of clustering have been proposed.[22–27] They are much more computationally efficient and can also be more accurate than clustering. In Ref.[27], a measurement-oriented sampling scheme is applied to sample particles, resulting in different particle subsets each corresponding to a specified measurement and a potential estimate; however, this MEE method will alter the particle-PHD recursions. Based on a data-driven viewpoint, the weight of particles is attributed to measurements, and therefore can be partitioned with respect to measurement for MEE.[22–26]

Existing MEE solutions based on either the integrated weight or weight components essentially extract the local supreme of the PHD as state-estimates which, however, omit the correlation between detected targets and are therefore "biased," although the correlation is of little practical significance for general except for closely spaced targets.[28] This inherent correlation is similar to the coalescence effect that occurs with the closely-spaced targets in traditional M2T association-based MTT solutions.[29–31] A good MEE solution will make the best effort to reduce this correlation in order to maximally match the independence between targets. It is argued in Ref.[32] that "for the limited number of particles used in practice, PFs that assume posterior independence among target states outperform those without it." To date, an engineer-friendly MEE method that is reliable, accurate and computationally fast is crucial, but still missing for the SMC-PHD filter despite extensive efforts devoted in this regard.

In this paper, we leverage the posterior independence approximation and recall decision and association techniques to formulate the SMC-PHD MEE problem as a set of parallel single-target state-estimation problems, which will maximally reduce the correlation/bias among estimates and enable the use of the optimal EAP (Expected a Posteriori) estimator. The proposed MEE approach, termed the Multi-EAP (MEAP) estimator, is free of iterative clustering computation and therefore computes quickly and reliably.

This remainder of paper is arranged as follows: Section 2 - key notations used and related works; Section 3 – details of the proposed MEAP estimator; Section 4 - simulation comparison of the MEAP approach with state-of-the-art MEE methods; Section 5 - conclusion.

2. Problem statement and related works

Basically, MEE is carried out on the filtering posterior that will not affect the recursions of the filter. Because of this, this paper

Please cite this article in press as: Li T et al. Multi-EAP: Extended EAP for multi-estimate extraction for SMC-PHD filter, *Chin J Aeronaut* (2017), http://dx.doi.org/10.1016/j.cja.2016.12.025

is only concerned with the variables involved in the posterior while the details of filtering recursions are omitted. This allows a clear and easy understanding of our approach. For the details of the default PHD filter and its SMC implementation, the reader is referred to Refs.[5,11,12]. The concerned variables are denoted as follows:

k, time-instant (positive integer),
$\boldsymbol{X}_k = \{\boldsymbol{x}_{k,1}, \boldsymbol{x}_{k,2}, \ldots, \boldsymbol{x}_{k,N_k}\}$, RFS of the states of all targets, where N_k is the number of targets,
$\boldsymbol{Z}_k = \{\boldsymbol{z}_{k,1}, \boldsymbol{z}_{k,2}, \ldots, \boldsymbol{z}_{k,M_k}\}$, RFS of the measurements where M_k is the number of measurements, consisting of two disjoint RFSs: target-originated measurement RFS $\boldsymbol{Z}_{k,\mathrm{T}}$ and clutter RFS $\boldsymbol{Z}_{k,\mathrm{C}}$, satisfying $\boldsymbol{Z}_k = \boldsymbol{Z}_{k,\mathrm{T}} \cup \boldsymbol{Z}_{k,\mathrm{C}}$,
L_k, number of particles at time k (specifically at the filtering updating stage),
$\boldsymbol{x}_k^{(i)}$, state of particle i at time $k, i \in [1, L_k]$,
$w_k^{(i)}$, the posterior weight of particle i at time k, obtained after PHD updating,
$w_{k|k-1}^{(i)}$, the prior weight of particle i at time k, obtained after PHD prediction,
$\delta_{\boldsymbol{y}}(\boldsymbol{x})$, Dirac delta function, which equals to one if $\boldsymbol{x} = \boldsymbol{y}$ and to zero otherwise,
$p_{\mathrm{D},k}(\boldsymbol{x})$, detection probability of a target with state $\boldsymbol{x}$ at time k,
κ_k, clutter intensity at time k,
$g_k(\boldsymbol{z}|\boldsymbol{x})$, likelihood of measurement $\boldsymbol{z}$ conditioned on state $\boldsymbol{x}$,
$H(\boldsymbol{x})$, measurement function.

2.1. RFS filtering and the PHD recursion

A RFS variable is a random variable that takes values as unordered finite sets. The cardinality of a RFS variable $\boldsymbol{X}$ is random and modelled by a discrete distribution $\rho(n) = \Pr\{|\boldsymbol{X}| = n\}$, where n is a non-negative integer. The RFS $\boldsymbol{X}$ is specified entirely by its cardinality distribution $\rho(n)$ and a family of symmetric joint distributions $p_n(\boldsymbol{x}_1, \boldsymbol{x}_2, \ldots, \boldsymbol{x}_n)$ that characterize the distribution of its elements over the state space, conditioned on the set cardinality n. Here, a joint distribution function $p_n(\boldsymbol{x}_1, \boldsymbol{x}_2, \ldots, \boldsymbol{x}_n)$ is said to be symmetric if its value remains unchanged for all of the $n!$ possible permutations of its variables. The PDF (probability density function) of an RFS variable $\boldsymbol{X}$ is denoted $f(\boldsymbol{X})$ and defined as $f(\{\boldsymbol{x}_1, \boldsymbol{x}_2, \ldots \boldsymbol{x}_n\}) = n! \cdot \rho(n) \cdot p_n(\boldsymbol{x}_1, \boldsymbol{x}_2, \ldots \boldsymbol{x}_n)$.

The RFS theory provides an exquisite tool to represent the unknown and size-varying state set and measurement set involved in the MTT scene. While representing targets and measurements as RFSs, we need an alternative Bayes-Markov filter that is able to handle set densities in order to deal with multi-target tracking. To this end, the multi-target Bayesian filter is given by two equations for prediction and Bayes updating, respectively, as follows[2–5]:

$$p(\boldsymbol{X}_k|\boldsymbol{Z}_{1:k-1}) = \int p(\boldsymbol{X}_k|\boldsymbol{X}_{k-1}) p(\boldsymbol{X}_{k-1}|\boldsymbol{Z}_{1:k-1}) \mathrm{d}\boldsymbol{X}_{k-1} \tag{1}$$

$$p(\boldsymbol{X}_k|\boldsymbol{Z}_k) = \frac{p(\boldsymbol{Z}_k|\boldsymbol{X}_k) p(\boldsymbol{X}_k|\boldsymbol{Z}_{1:k-1})}{p(\boldsymbol{Z}_k|\boldsymbol{Z}_{1:k-1})} \tag{2}$$

where $p(\boldsymbol{Z}_k|\boldsymbol{Z}_{1:k-1}) = \int p(\boldsymbol{Z}_k|\boldsymbol{X}_k) p(\boldsymbol{X}_k|\boldsymbol{Z}_{1:k-1}) \mathrm{d}\boldsymbol{X}_k$ and the integrals are set integrals defined as

$$\int p(\boldsymbol{X}) \mathrm{d}\boldsymbol{X} = p(\varnothing) + \sum_{n=1}^{\infty} \frac{1}{n!} \int p(\{\boldsymbol{x}_1, \boldsymbol{x}_2, \ldots, \boldsymbol{x}_n\}) \mathrm{d}\boldsymbol{x}_1 \mathrm{d}\boldsymbol{x}_2 \ldots \mathrm{d}\boldsymbol{x}_n \tag{3}$$

Unfortunately, the above full Bayesian equations involve the calculation of set integrals and cannot be analytically solved except for very few special cases. Instead of propagating the complete multi-target density, the PHD filter propagates its first order moment, called the intensity function or PHD, which calculates the distribution that minimizes the set KLD to approximate the multi-target Bayesian posterior within the Poisson point process family.[6,7] This filter was originally derived using probability generating functionals and functional derivatives.[5] Alternative derivations for the PHD filter based on measure theory have been proposed in Refs.[33,34] This has also motivated a variety of new interpretations and implementations (see Refs.[20,35–37]).

The following assumptions are required in the classic PHD filter.[16].

Assumption 1. Each target evolves and generates measurements independently of others.

Assumption 2. The clutter distribution is Poisson and independent of the target-generated measurements.

Assumption 3. One target can generate no more than one measurement at each scan.

Assumption 4. The number of new appearing targets at each scan is a Poisson random variable and is independent of the existing targets.

Assumption 5. Both the surviving-target process and the target-generated measurement process are Bernoulli.

For a given RFS Ξ with the multi-target probability density function $f_{\Xi}(\boldsymbol{X})$, the PHD $D_{\Xi}(\boldsymbol{x})$ is given as:

$$D_{\Xi}(\boldsymbol{x}) = \int \delta_{\boldsymbol{X}}(\boldsymbol{x}) f_{\Xi}(\boldsymbol{X}) \mathrm{d}\boldsymbol{X} \tag{4}$$

where $\delta_{\boldsymbol{X}}(\boldsymbol{x}) \triangleq \sum_{\boldsymbol{w} \in \boldsymbol{X}} \delta_{\boldsymbol{w}}(\boldsymbol{x})$ is the set Dirac delta function, respectively, which is used to convert the finite set $\boldsymbol{X} = \{\boldsymbol{x}_1, \boldsymbol{x}_2, \ldots\}$ into vectors since the first order statistical moment is defined in the vector space. We have the cardinality of an RFS $\boldsymbol{X}$ as $|\boldsymbol{X}| = \int \delta_{\boldsymbol{X}}(\boldsymbol{x}) \mathrm{d}\boldsymbol{x}$.

In this paper, we investigate the classic SMC-PHD filter[11,12] for clarity, although the proposed MEE approach is not limited to this. The PHD predictor (time updating) is

$$D_{k|k-1}(\boldsymbol{x}) = \int \phi_{k|k-1}(\boldsymbol{x}|\boldsymbol{u}) D_{k-1|k-1}(\boldsymbol{u}) \mathrm{d}\boldsymbol{x} + \gamma_k(\boldsymbol{x}) \tag{5}$$

where the following abbreviation is used

$$\phi_{k|k-1}(\boldsymbol{x}|\boldsymbol{u}) = p_{\mathrm{s},k}(\boldsymbol{u}) f_{k|k-1}(\boldsymbol{x}|\boldsymbol{u}) + b_k(\boldsymbol{x}|\boldsymbol{u}) \tag{6}$$

where $p_{\mathrm{s},k}(\boldsymbol{u})$ is the probability that the target with state $\boldsymbol{u}$ survive at time k and transition to some other (random) state, $b_k(\boldsymbol{x}|\boldsymbol{u})$ denotes the intensity function of the RFS of targets spawned from the previous state u, and $\gamma_k(\boldsymbol{x})$ is the birth inten-

sity function of new targets at time k. $D_{k-1|k-1}(\boldsymbol{x})$ is the posterior PHD at time $k-1$ and is given as follows for time k.

The PHD updater (data updating) is

$$D_{k|k}(\boldsymbol{x}) = \left(1 - p_{\mathrm{D},k}(\boldsymbol{x}) + \sum_{z\in\boldsymbol{Z}_k} \frac{p_{\mathrm{D},k}(\boldsymbol{x}) g_k(\boldsymbol{z}|\boldsymbol{x})}{\kappa_k(\boldsymbol{z}) + C_k(\boldsymbol{z})}\right) D_{k|k-1}(\boldsymbol{x}) \tag{7}$$

with the abbreviation

$$C_k(\boldsymbol{z}) = \int p_{\mathrm{D},k}(\boldsymbol{u}) g_k(\boldsymbol{z}|\boldsymbol{u}) D_{k|k-1}(\boldsymbol{u}) \mathrm{d}\boldsymbol{u} \tag{8}$$

2.2. Weight component of particles

As addressed, MEE is performed with the posterior PHD, which allows us to start directly with the particle approximation of the PHD updater $D_{k|k}$

$$D_{k|k}(\boldsymbol{x}_k) \approx \sum_{i=1}^{L_k} w_k^{(i)} \delta_{\boldsymbol{x}_k^{(i)}}(\boldsymbol{x}_k) \tag{9}$$

with the posterior weight given as

$$w_k^{(i)} = \left[1 - p_{\mathrm{D},k}\left(\boldsymbol{x}_k^{(i)}\right) + \sum_{z\in\boldsymbol{Z}_k} \frac{p_{\mathrm{D},k}\left(\boldsymbol{x}_k^{(i)}\right) g_k(\boldsymbol{z}|\boldsymbol{x}_k^{(i)})}{\kappa_k + \sum_{j=1}^{L_k} p_{\mathrm{D},k}\left(\boldsymbol{x}_k^{(j)}\right) g_k(\boldsymbol{z}|\boldsymbol{x}_k^{(j)}) w_{k|k-1}^{(j)}}\right] w_{k|k-1}^{(i)} \tag{10}$$

As shown in Eq. (10), the (posterior) weights consist of two parts. One part corresponds to misdetection (we denote it as $\boldsymbol{z}_0$ for easy addressment) and the other part to target-generated measurements and clutter $\boldsymbol{z} \in \boldsymbol{Z}_k$. Thus, the "weight component" can be defined as[13]:

$$w_k^{(i)}(\boldsymbol{z}) = \begin{cases} \left(1 - p_{\mathrm{D},k}\left(\boldsymbol{x}_k^{(i)}\right)\right) w_{k|k-1}^{(i)} & \text{if } \boldsymbol{z} = \boldsymbol{z}_0 \\ \dfrac{p_{\mathrm{D},k}\left(\boldsymbol{x}_k^{(i)}\right) g_k(\boldsymbol{z}|\boldsymbol{x}_k^{(i)}) w_{k|k-1}^{(i)}}{\kappa_k + \sum_{j=1}^{L_k} p_{\mathrm{D},k}\left(\boldsymbol{x}_k^{(j)}\right) g_k(\boldsymbol{z}|\boldsymbol{x}_k^{(j)}) w_{k|k-1}^{(j)}} & \text{if } \boldsymbol{z} \in \boldsymbol{Z}_k \end{cases} \tag{11}$$

This gives an index of how much each $\boldsymbol{z}$ contributes to the weight of particle i.

Obviously, we have

$$w_k^{(i)} = \sum_{z\in\{\boldsymbol{z}_0,\boldsymbol{Z}_k\}} w_k^{(i)}(\boldsymbol{z}) \tag{12}$$

We further denote

$$W_k(\boldsymbol{z}) := \sum_{i=1}^{L_k} w_k^{(i)}(\boldsymbol{z}) \tag{13}$$

which gives an indication about the probability that the underlying measurement is from a real target ($\boldsymbol{z}\in\boldsymbol{Z}_k$) or the expectation that misdetection occurs ($\boldsymbol{z}=\boldsymbol{z}_0$).

Lemma 1 [36]. $\forall \boldsymbol{z} \in \boldsymbol{Z}_k : 0 \leqslant W_k(\boldsymbol{z}) \leqslant 1$.

Proof. By substituting Eq. (11) into Eq. (13) under the condition $\boldsymbol{z} \in \boldsymbol{Z}_k$, $W_k(\boldsymbol{z})$ can be expanded as

$$W_k(\boldsymbol{z}) = \sum_{i=1}^{L_k} \frac{p_{\mathrm{D},k}\left(\boldsymbol{x}_k^{(i)}\right) g_k(\boldsymbol{z}|\boldsymbol{x}_k^{(i)}) w_{k|k-1}^{(i)}}{\kappa_k + \sum_{j=1}^{L_k} p_{\mathrm{D},k}\left(\boldsymbol{x}_k^{(j)}\right) g_k(\boldsymbol{z}|\boldsymbol{x}_k^{(j)}) w_{k|k-1}^{(j)}} \in [0,1]$$

To have the extremes of the interval on the right side, when and only when $p_{\mathrm{D}}(\boldsymbol{x}) = 0$, $W_k(\boldsymbol{z}) = 0$, and when and only when $\kappa_k(\boldsymbol{z}) = 0$, $W_k(\boldsymbol{z}) = 1$.

The PHD is uniquely defined by the property that its integral in any region indicates the expected number of targets in that region. That is, the integration of the PHD over the entire state space gives the expected number of targets. Therefore, a common approach to estimate the number of targets N_k is rounding the total weight sum as

$$\widehat{N}_k = \left[\sum_{i=1}^{L_k} w_k^{(i)}\right] \tag{14}$$

which is a near-EAP estimation.[5,21] □

2.3. Weight component-based MEE

In order to extract multiple estimates from the PHD, decomposition is needed for MEE that can be carried out either on the particles or on their weights. In the former, the clustering partitions particles into different groups, each corresponding to a target. In the latter, the weights of particles are decomposed with respect to measurements, as implied by Eq. (11), and then the weight components are used to calculate estimates. In this regard, Zhao[22] selects $\widehat{N}_k$ measurements from $\{\boldsymbol{z}_0, \boldsymbol{Z}_k\}$ with the largest $W_k(\boldsymbol{z})$ (called the *Rank* rule hereafter) and for each $\boldsymbol{z} \in \{\boldsymbol{z}_0, \boldsymbol{Z}_k\}$, an estimate is obtained as the component-weighted mean of the states of all particles

$$\boldsymbol{x}_k^{\mathrm{Zhao}}(\boldsymbol{z}) = \frac{\sum_{i=1}^{L_k} w_k^{(i)}(\boldsymbol{z}) \boldsymbol{x}_k^{(i)}}{W_k(\boldsymbol{z})} \tag{15}$$

In contrast, Ristic[23,24] proposes to extract estimates from $\boldsymbol{z} \in \{\boldsymbol{z}_0, \boldsymbol{Z}_k\}$ if its contribution $W_k(\boldsymbol{z})$ is bigger than a specified threshold W_{T} (hereafter referred to as the *Threshold* rule). This eliminates the need to estimate the cardinality $\widehat{N}_k$. The state-estimate corresponding to the selected $\boldsymbol{z}$ is given as

$$\boldsymbol{x}_k^{\mathrm{Ristic}}(\boldsymbol{z}) = \sum_{i=1}^{L_k} w_k^{(i)}(\boldsymbol{z}) \boldsymbol{x}_k^{(i)} \tag{16}$$

As a key difference from Eq. (15), the weight is not normalized in Eq. (16). The failure of normalization is corrected by Refs.[25,26], which, in addition, do not take new-born particles into account. The estimate is then calculated as follows:

$$\boldsymbol{x}_k^{\mathrm{Schikora}}(\boldsymbol{z}) = \frac{\sum_{i=1}^{L_{k-1}} w_k^{(i)}(\boldsymbol{z}) \boldsymbol{x}_k^{(i)}}{\sum_{i=1}^{L_{k-1}} w_k^{(i)}(\boldsymbol{z})} \tag{17}$$

where L_{k-1} denotes the number of particles that are transited from time $k-1$ which excludes the new generated particles at time k.

Assuming that J_k new particles are allocated for new targets at time k, we have $L_k = L_{k-1} + J_k$. Obviously, the outcome of Eq. (17) is very close to that of Zhao's method as given in Eq. (15). This group of solutions employs weight components to extract estimates, which as will be demonstrated in our simulations can produce much better accuracy and compute faster than clustering.

Please cite this article in press as: Li T et al. Multi-EAP: Extended EAP for multi-estimate extraction for SMC-PHD filter, *Chin J Aeronaut* (2017), http://dx.doi.org/10.1016/j.cja.2016.12.025

2.4. Correlation between detected targets

When extracting state-estimates of individual targets from the PHD, the local peaks are often unstable, resulting in an abundance of practical difficulties. First, when two or more targets coalesce into one intensity peak, it is not clear how to proceed. Second, a nontrivial theoretical objection is that the intensity (number of targets per unit state space) is a summary statistic and not a full multi-target PDF, so the meaning of estimates obtained from the intensity are of unknown statistical character.[38] More importantly, as implied by Eq. (10), the weights of particles are contributed to by all measurements (including that of all targets) as are the resultant estimates correlatively based on them. MEE methods that do not compensate for the correlation between detected targets are theoretically biased, although the bias is of little practical significance in many situations.[28] In order to best comply with the reality, our approach is developed on the basis of posterior independence approximation and does not use the multi-target posterior weight Eq. (10) of particles; rather, each estimate is calculated with respect to partitioned subsets of particles and independent measurements. As the core idea to reduce correlation between detected targets, particles are divided with respect to all of the measurements (including clutter) rather than only to tracks/estimates. This is preferable if we consider that some particles are generated and weighted primarily because of clutter rather than real measurements and therefore shall not be associated to any estimate. The "divide" idea sits on the same ground as the M2T association carried out in traditional MTT approaches. By these proper data association techniques, the MEE problem is formulated as a set of parallel sub-problems of single-estimate extraction; each sub-problem that consists of one measurement and a sub-group of particles extracts one estimate optimally and individually. Further discussion is given in Section 3.4.

3. MEAP estimator

In brief, the particles will be associated with different measurements (using the near and nearest neighbor, NNN, rule; see Section 3.1), while the measurements will be distinguished between those generated by targets and clutter based on Eq. (12) (see Section 3.2). Each measurement that is identified to be generated by a real target and its associated particles will be handled independently to extract one estimate in the EAP estimation (see Section 3.3).

3.1. NNN particle-to-measurement (P2M) association

Although the PHD filter updates the weight of each particle by using all measurement information, only close measurements dominate, determining the existence of that particle, and small weighted particles are abandoned in the resampling process.[39] Therefore, it is preferable to use only the particles that are close to the underlying measurement for the corresponding single-estimate calculation in order to maximally reduce the correlation among different estimates.

At first, we adopt the nearest neighbor (NN) rule to divide the particles with regard to their space proximity according to individual measurements. For example, in Fig. 1(a), (b) and (c) for the case of two measurements (marked by "+") with different distances, the particles (marked by dots) are associated with their nearest measurement and marked in different colors (red or green). However, when two or more measurements are very close, the particles are highly mixed and the NN association is not really effective at dealing with the correlation. For example in Fig. 1(c), two measurements almost overlap; each measurement is then associated with only half the number of the particles in the joint cloud by using the NN association. The resulting estimates are likely to drift away from the center as they omit the particles on the other side in their calculation, even if those particles (e.g. the ones distributed in the circles) are very close to them. This exposes one of the shortcomings of the standard NN association, which is limited to "one-to-one" association. The same occurs in cases when more targets are close to each other.

Taking this specific case into account, we extend the NN method to include the very near (though not the nearest) particles that are not associated with the underlying measurement according to the NN principle, namely the NNN-based P2M association rule, which can be written as:

$$\Xi(\boldsymbol{z}) = N(\boldsymbol{z}) \bigcup G(\boldsymbol{z}) \tag{18}$$

where $N(\boldsymbol{z})$ is the index set of particles whose nearest measurement is $\boldsymbol{z}$ and $G(\boldsymbol{z})$ is the index set of particles that lie in the validation area specified by an elliptical gate around measurement $\boldsymbol{z}$. They can be written as

$$N(\boldsymbol{z}) = \left\{ i \middle| \boldsymbol{z} = \mathrm{argmin}_{\boldsymbol{a} \in \boldsymbol{Z}_k} \left\| \boldsymbol{a} - H\left(\boldsymbol{x}_k^{(i)}\right) \right\|_2, i = 1, 2, \ldots, L_k \right\} \tag{19}$$

$$G(\boldsymbol{z}) = \left\{ i \middle| \left(\boldsymbol{z} - H\left(\boldsymbol{x}_k^{(i)}\right)\right)^{\mathrm{T}} \boldsymbol{R}^{-1} \left(\boldsymbol{z} - H\left(\boldsymbol{x}_k^{(i)}\right)\right) \leqslant \mathcal{T}, i = 1, 2, \ldots, L_k \right\} \tag{20}$$

where $\mathcal{T}$ is a gate threshold, which shall be properly designed in order to capture the significant particles while not overshooting, and $\boldsymbol{R}$ is the measurement noise covariance. As $G(\boldsymbol{z})$ serves mainly to remedy the NN rule, we suggest a small magnitude of 0.5–2. To note, $N(\boldsymbol{z})$ and $G(\boldsymbol{z})$ are not necessarily disjointed.

3.2. Distinguishing measurements

The state of targets evolves in a Markov process while the clutter does not necessarily evolve with the same process over time.

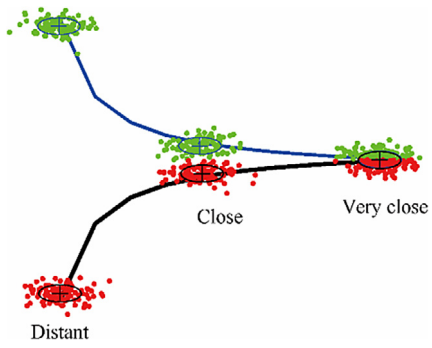

Fig. 1 Different space proximities of measurements for two targets and the particle-to-measurement NN association.

This core difference intuitively forms a criterion to distinguish the real measurements generated by targets from clutter: the former is more likely to fall in areas of higher PHD where the mass of weighted particles is relatively larger. Therefore, we have:

Criterion 1. The measurements that contribute more significantly to the PHD, in terms of corresponding to relatively larger $W_k(\boldsymbol{z})$, are more likely generated by targets.

This criterion has actually been employed in two different manners in existing measurement-oriented MEE methods: Ristic's Threshold rule[23] and the Rank rule as seen in Refs.[22,24–26]. In our approach, we can employ either the Threshold rule or the Rank rule to determine the potential target measurement RFS $\boldsymbol{Z}_{k,\mathrm{T}} \subseteq \boldsymbol{Z}_k$; then EAP will be applied as shown in the next subsection. The rules correspond to Algorithm 1 and 2 respectively, and are referred to as MEAP 1 and MEAP 2; the latter is also treated as the default MEAP estimator.

3.3. EAP estimator

The Bayes' theorem indicates that $p(\boldsymbol{x}|\boldsymbol{z}) \propto p(\boldsymbol{z}|\boldsymbol{x})p(\boldsymbol{x})$, namely "posterior is proportional to prior times likelihood." In our case, for each potential target-originated measurement $\boldsymbol{z} \in \boldsymbol{Z}_{k,\mathrm{T}}$ and the corresponding NNN associated particle set $\Xi(\boldsymbol{z})$ obtained in the preceding two steps, it is straightforward that the single-target posterior weight of the particle (normalized over the set $\Xi(\boldsymbol{z})$) can be defined as:

$$\varpi_{\boldsymbol{z}}^{(i)} = \frac{g_k\left(\boldsymbol{z}|\boldsymbol{x}_k^{(i)}\right) w_{k|k-1}^{(i)}}{\sum_{i\in\Xi(\boldsymbol{z})} g_k\left(\boldsymbol{z}|\boldsymbol{x}_k^{(i)}\right) w_{k|k-1}^{(i)}} \tag{21}$$

Then, one EAP state-estimate (which is the mean of the posterior distribution)[40] can be extracted, just as is done in the standard single-measurement single-target case, by

$$\boldsymbol{x}_k^{\mathrm{EAP}}(\boldsymbol{z}) = \sum_{i\in\Xi(\boldsymbol{z})} \boldsymbol{x}_k^{(i)} \varpi_{\boldsymbol{z}}^{(i)} \tag{22}$$

with the estimation variance

$$\mathrm{Cov}\left(\boldsymbol{x}_k^{\mathrm{EAP}}(\boldsymbol{z})\right) = \sum_{i\in\Xi(\boldsymbol{z})} \varpi_{\boldsymbol{z}}^{(i)} \left(\boldsymbol{x}_k^{(i)} - \boldsymbol{x}_k^{\mathrm{EAP}}(\boldsymbol{z})\right)\left(\boldsymbol{x}_k^{(i)} - \boldsymbol{x}_k^{\mathrm{EAP}}(\boldsymbol{z})\right)^{\mathrm{T}} \tag{23}$$

To note, the calculation of the likelihood $g_k\left(\boldsymbol{z}|\boldsymbol{x}_k^{(i)}\right)$ that is relatively computationally intensive does not need to be repeated, as one can directly use the result obtained in Eq. (10) when the particle weight is updated. This speedup is feasible because the MEE is always performed at the end of the filtering in each iteration.

If there is only one target and one measurement (in other words, neither misdetection nor clutter is involved), MEAP will reduce to the standard optimal EAP that minimizes the mean square error of the estimation,[40] as briefly shown in Lemma 2.

Lemma 2. The EAP estimate minimizes the mean square error of the estimation defined as (ℓ_2 norm)

$$\sum_{i\in\Xi(\boldsymbol{z})} \varpi_{\boldsymbol{z}}^{(i)} \left\|\boldsymbol{x}_k^{(i)} - \boldsymbol{x}_k^{\mathrm{EAP}}\right\|_2^2 \tag{24}$$

Proof. Setting the derivative of Eq. (24) as zero yields $\sum_{i\in\Xi(\boldsymbol{z})} \varpi_{\boldsymbol{z}}^{(i)} \left(\boldsymbol{x}_k^{(i)} - \boldsymbol{x}_k^{\mathrm{EAP}}\right) = \boldsymbol{0}$, which gives the MMSE estimate Eq. (22), i.e., the mean square error of the estimation given in Eq. (24) is minimized by Eq. (22). □

The final output of MEAP is a local approximation of the MMSE, ignoring misdetections and the effect of clutter. However the estimated number of targets if given in Eq. (14) by the Rank rule is near-EAP (see the derivation given in Ref.[5]), while if given by the Threshold rule it is ad hoc. Overall, the MEAP 2 estimator is approximately locally optimal (the more distant estimates are with each other and the less misdetection, the closer to optimal the result), while MEAP 1 is simply an ad hoc solution due to the threshold used. Further discussion will be given with the simulation results in Section 4. □

In summary, the proposed MEAP estimators consist of three main steps:

Step 1. (Criterion 1) distinguish the real measurement of targets $\boldsymbol{Z}_{k,\mathrm{T}}$ from clutter based on $W_k(\boldsymbol{z})$.
Step 2. (NNN association) associate the particles to their nearest and near measurement(s).
Step 3. (EAP estimator) extract the EAP state-estimates with respect to each real measurement $\boldsymbol{z} \in \boldsymbol{Z}_{k,\mathrm{T}}$ and its locally associated particles.

Algorithm 1. MEAP 1.

```
FOR z ∈ Z_k DO
    IF W_k(z) ⩾ W_T DO
        Extract one estimate via Eq. (22)
```

Algorithm 2. MEAP 2.

```
FOR j = 1, 2, ..., min(N̂_k, |Z_k|) DO
    z = argmax_{a∈Z_k} W_k(a)
    Extract one estimate via Eq. (22)
    W_k(a) ← 0
```

3.4. Remarks

Apparently, the proposed MEAP estimators resemble the measurement-oriented methods[22–26] in that they all extract estimates by taking measurements into account individually, and are suitable for parallel processing[36] due to measurement independence. This is also an important property of the proposed MEAP estimator, which is superior to most clustering methods. However, a core difference between the MEAP estimator and the others is that the calculation of each estimate is not based on the posterior weight $w_k^{(i)}$ or its component $w_k^{(i)}(\boldsymbol{z})$ of particles that admit correlation among particles, as shown in the summation calculation in the denominator of Eq. (10)/Eq. (11). Moreover, the NNN rule will filter out the unrelated particles (including those that exist more likely because of clutter or other targets), not using them in the state-estimate calcu-

lation of the underlying target. Once the decision and association have been carried out, the final EAP calculation is independent of the target detection probability and the clutter intensity. In other words, the state of targets is independent. On this point, we need to be clear on the difference between the PHD filtering and MEE, and the independence between targets. This forms the theoretical basis of our "divide-and-conquer" solution. We posit the following remarks:

Remark 1. Criterion 1 is restrictive as clutter may fall close to existing particles, thereby giving significant rise to the PHD, and will be taken as a target. In this case, even the PHD itself will be locally over-estimated (generating false alarms) and the MEE (applying to all existing methods) cannot be any better. This is an inherent drawback of the PHD updator that is based on measurement of single-frame only.

Remark 2. In the PHD updater, the misdetection of targets is compensated by the posterior of the preceding iteration, which, however, gives no indication as to which target was missed. In existing works that use the mean of the PHD as the estimate, e.g. Refs.[22–24], it does not make sense to extract any target, unless there is exactly one target in total and it was missed in detection. In contrast, Refs.[25,26] report no estimate for missed targets, just as is done in our approach.

One possible solution to deal with misdetections is to create pseudo measurements[41] for missed targets so that the MEAP estimator can be employed within. More generally, one may consider filling the misdetection or removing isolated false alarms based on the information of successive frames[21,30,42–44] or even maintaining a representation of targets that have never been detected.[45] In our current implementation based on single frame information, the basic MEAP estimator will not report any state-estimate for missed targets, but it leaves the decision to subsequent track management using the information of successive frames[44] or to say the history information.[46] Further improvements include using the particle path instead of the single scan state[31] or labelling particles,[44,46] and to jointly solve MEE with track management.[3].

Remark 3. For multi-model tracking of maneuvering targets (e.g., Ref.[47]), the particles as well as the targets are associated with different models. To apply the MEAP method in this case, the NNN association takes the target model into account so that only particles of the same model as the involved target should be considered.

4. Simulations

The key performance assessment for MEE shall account for accuracy, computational efficiency and reliability. In our simulations, the most widely used k-means algorithm (which runs up to 50 iterations if the algorithm does not converge), Ristic's method,[23], Zhao's method[22] and the proposed estimators MEAP 1 and 2 are independently applied on the same filter. The number of targets is estimated online in Ristic's method and MEAP 1 by using the same threshold $W_{\mathrm{T}} = 0.6$ while the same $\widehat{N}_k$ as given in Eq. (14) is used in the other three methods. In the best effort to provide fair comparisons, two typical simulation models with different degrees of scenario complexity are employed. To capture the average performance, we apply a large range of clutter rates and run 100 Monte Carlo trials.

The optimal sub-pattern assignment (OSPA) metric[48] is used to evaluate the estimation accuracy of the filter. A large OSPA metric indicates a low accuracy. For two finite subsets $\boldsymbol{X} = \{\boldsymbol{x}_1, \boldsymbol{x}_2, \ldots, \boldsymbol{x}_m\}$ and $\boldsymbol{Y} = \{\boldsymbol{y}_1, \boldsymbol{y}_2, \ldots, \boldsymbol{y}_n\}$ where $m, n \in \mathbf{N}_0 = \{0, 1, 2, \ldots\}$, the OSPA metric of order p between $\boldsymbol{X}$ and $\boldsymbol{Y}$ is defined as (if $m \leqslant n$):

$$\bar{d}_p^{(c)}(\boldsymbol{X}, \boldsymbol{Y}) = \left(\frac{1}{n} \left(\min_{\pi \in \Pi_n} \sum_{i=1}^{m} d^{(c)}(\boldsymbol{x}_i, \boldsymbol{y}_{\pi(i)})^p + c^p(n-m) \right) \right)^{1/p} \tag{25}$$

where $d^{(c)}(\boldsymbol{x}, \boldsymbol{y}) = \min(c, d(\boldsymbol{x}, \boldsymbol{y}))$, the cut off parameter $c > 0$ and $d(\boldsymbol{x}, \boldsymbol{y})$ is the Euler distance. $\bar{d}_p^{(c)}(\boldsymbol{X}, \boldsymbol{Y}) = \bar{d}_p^{(c)}(\boldsymbol{Y}, \boldsymbol{X})$ if $m > n$ and $\bar{d}_p^{(c)}(\boldsymbol{X}, \boldsymbol{Y}) = 0$ if $m = n = 0$.

The order parameter p determines the sensitivity to outliers, and the cut-off parameter c determines the relative weighting of the penalties assigned to cardinality and localization errors. In general, the parameter p is often chosen as 1 or 2 while the cut-off parameter c is designed according to the size of the scenario. In both of our simulations we set $p = 2$, but $c = 100$ in the first simulation with a smaller scenario and $c = 500$ in the second simulation with a larger scenario.

4.1. Nearly constant velocity target dynamics

The simulation is designed in a two-dimensional scenario over the region $[-100, 100] \times] - 100, 100]$ m^2. The trajectories of targets are shown in Fig. 2. It is known that new targets appear according to a Poisson point process with intensity function $\gamma_k = 0.2\mathcal{N}(.; \bar{\boldsymbol{x}}, \boldsymbol{Q})$, where $\bar{\boldsymbol{x}} = [-50, 3, 50, -3]^{\mathrm{T}}$, $\boldsymbol{Q} = \mathrm{diag}([10, 1, 10, 1]^{\mathrm{T}})$ ($\mathrm{diag}(\boldsymbol{a})$ gives a diagonal matrix with diagonal $\boldsymbol{a}$). The single target Markov transition that characterizes the constant velocity target dynamics is given as:

$$\boldsymbol{x}_k = \begin{bmatrix} 1 & \Delta & 0 & 0 \\ 0 & 1 & 0 & 0 \\ 0 & 0 & 1 & \Delta \\ 0 & 0 & 0 & 1 \end{bmatrix} \boldsymbol{x}_{k-1} + \boldsymbol{V}_k \tag{26}$$

where $\Delta = 1$ s is one sampling interval, $\boldsymbol{V}_k$ is a zero-mean Gaussian vectors with covariance

$$\boldsymbol{\Sigma}_k = \begin{bmatrix} \Delta^3/3 & \Delta^2/2 & 0 & 0 \\ \Delta^2/2 & \Delta & 0 & 0 \\ 0 & 0 & \Delta^3/3 & \Delta^2/2 \\ 0 & 0 & \Delta^2/2 & \Delta \end{bmatrix} l$$

where $l = 1 \times 10^{-4}$ m^2 s^{-3} is the level of the power spectral density of the corresponding process noise.

Three bearing sensors are located at $\left[s_{n,x}, s_{n,y}\right]^{\mathrm{T}}, n = 1, 2, 3$ that are $[-100, 100]^{\mathrm{T}}$, $[0, -100]^{\mathrm{T}}$ and $[100, 100]^{\mathrm{T}}$ respectively and the measurement equation is

$$z_{n,k} = \arctan\left(\frac{[\,1 \quad 0 \quad 0 \quad 0\,]\boldsymbol{x}_k - s_{n,x}}{[\,0 \quad 0 \quad 1 \quad 0\,]\boldsymbol{x}_k - s_{n,y}} \right) + w_{n,k} \tag{27}$$

where $\{w_{1,k}\}$, $\{w_{2,k}\}$ and $\{w_{3,k}\}$ are zero-mean Gaussian white noise with the same standard deviations of 0.05.

Parameters are set as $p_{\mathrm{S}}(\boldsymbol{x}) = 0.95$, $p_{\mathrm{D}}(\boldsymbol{x}) = 1$. In our case, under the condition that all sensors have the same unit

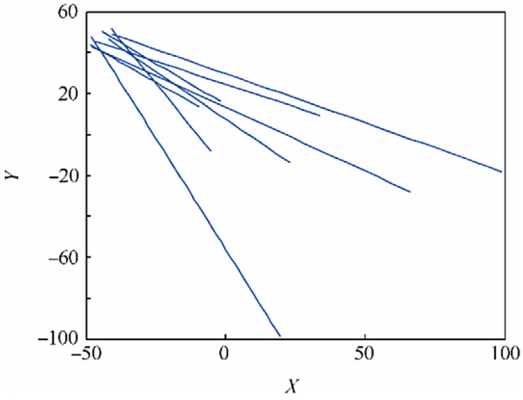

Fig. 2 Trajectories of targets born in the same area.

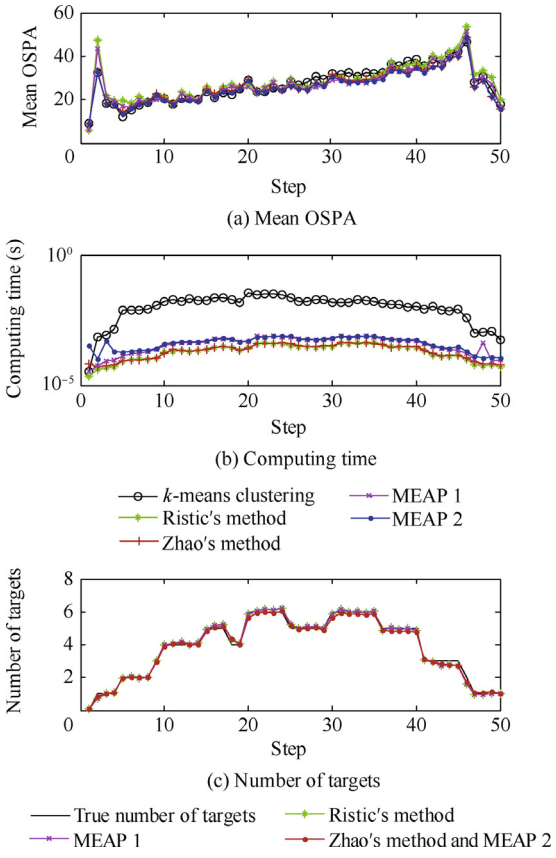

Fig. 3 Performance of different MEE methods when $r = 10$.

probability of detection, the final likelihood of the estimates is calculated by multiplying the single-sensor/target likelihoods obtained in all sensors. Clutter is uniformly distributed over the measurement space $[-\pi, -\pi/2]\times[-\pi/2, \pi/2]\times[\pi/2, \pi]$ with an average rate of r points per scan, i.e., a constant clutter density $\kappa_k = 4 \times r/\pi^3$. 500 particles per expected target are used and the total number of particles is hard-limited to be not less than 300. This is implemented via a minimum-sampling-variance (MSV) resampling procedure.[49]

First, we set the clutter rate $r = 10$. The mean OSPA, computing time, and estimated number of targets given by different MEE methods on the same filter are separately given in Fig. 3. The improvement of different methods in terms of the percentage that OSPA and computing time are reduced, as compared to the k-means clustering, is given in Table 1. Here, positive value indicates performance improvement (smaller OSPA and less computing time). Secondly, we apply a range of clutter rate r from 0 to 50. The mean OSPA and computing time reduced by the other methods as compared with the k-means method are given in Fig. 4. The results show:

(1) Ristic & Zhao's methods, MEAP 1 and 2, have obtained a similar, extremely fast computing speed that is significantly (greater than 95%) faster than the k-means clustering. This is because considerably less additional computations are required for their calculation, while the k-means clustering is a very time-consuming iteration procedure. Ristic and Zhao's methods are even faster than MEAP methods, as the latter additionally need to execute the particle-measurement NNN association.

(2) Ristic's method is inferior to other methods except for with very low clutter rate $r = 0$, 1, when it performs slightly better than the k-means method. The higher the clutter rate, the worse its performance. Meanwhile, the advantage of MEAP 1 over clustering is more obvious when the SNR (Signal-to-Noise Ratio) is high (e.g., $r < 10$), but clearly declines when the SNR is low. Extracting the same number of estimates at each step, MEAP 1 outperforms Ristic's method in estimation accuracy. The primary drawback of the latter as addressed is the lack of weight normalization. Better results might be obtained by utilizing another threshold W_T, which, however, is quite ad hoc.

(3) Notably, MEAP 2 has obviously yielded the highest accuracy of all methods for all stages. The advantage of MEAP 2 in terms of estimation accuracy over the k-means clustering tends to decrease with the growth of the clutter rate used. This is because many particles will be easily associated with clutter in cases of high clutter density, increasing the risk of generating false alarms. The smaller the clutter rate, the more accurate MEAP 2 becomes. When there is no clutter, MEAP 2 can reduce the OSPA by approximately 30% as compared with k-means; however, when there is heavy clutter (e.g., $r > 20$ in this case), MEAP 2 performs similar to k-means.

It is also worth noting that Zhao's method performs closely to the proposed MEAP 2 and outperforms the other methods

Table 1 Performance improvement of different MEE methods vs. k-means clustering when ($r = 10$).

Metric	Performance improvement (%)			
	Ristic's method	Zhao's method	MEAP 1	MEAP 2
OSPA	−4.1	3.2	1.1	4.9
Time	98.4	98.3	96.9	96.6

Please cite this article in press as: Li T et al. Multi-EAP: Extended EAP for multi-estimate extraction for SMC-PHD filter, *Chin J Aeronaut* (2017), http://dx.doi.org/10.1016/j.cja.2016.12.025

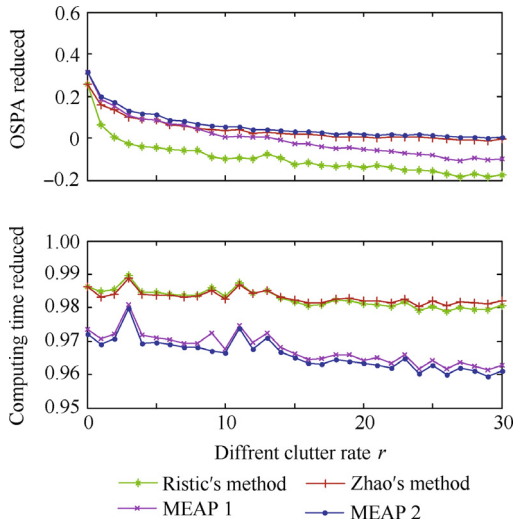

Fig. 4 Performance of different MEE methods for $r = 0$–50.

in most cases, although this does not seem to have attracted much attention in the field. This is not surprising as their calculations share high similarity, especially when the detection probability is high, the clutter intensity is low, and the targets are distant from one another; in such a case, their calculations are nearly the same mathematically. Regardless of the optimality of the EAP estimator, we reiterate that it is highly valuable to reduce the correlation as much as possible in order to comply with the reality that when targets are independent, so should be their state-estimates. Based on this line of thinking, the MEAP 2 approach does better both in theory and in practice.

4.2. Nearly constant turn-rate target dynamics

In this simulation, which is the same as that given in Ref.[8], new targets appear from four different areas as shown in Fig. 5. The range-and-bearing measurement region is a half disc of radius 2000 m. A target dynamic model having varying turn rate together with noisy bearings and range measurements is considered. The target state variable $\boldsymbol{x}_k = [p_{x,k}, \dot{p}_{x,k}, p_{y,k}, \dot{p}_{y,k}, \omega_k]^{\mathrm{T}}$ consists of the planar position $[p_{x,k}, p_{y,k}]^{\mathrm{T}}$ and velocity $[\dot{p}_{x,k}, \dot{p}_{y,k}]^{\mathrm{T}}$ and turn rate ω_k. The coordinated-turn state transition model can be written as:

$$\boldsymbol{x}_k = F(\omega_{k-1})\boldsymbol{x}_{k-1} + \boldsymbol{G}\boldsymbol{v}_{k-1} \tag{28}$$

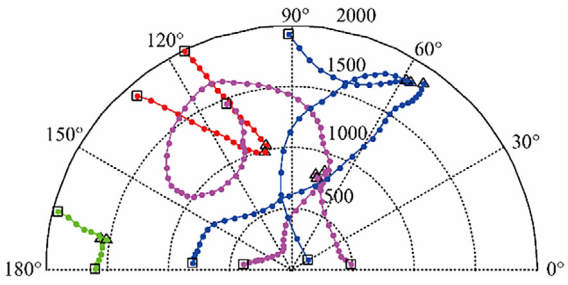

Fig. 5 Trajectories of targets born in four different areas.

where

$$F(\omega) = \begin{bmatrix} 1 & \omega^{-1}\sin(\omega\Delta) & 0 & \omega^{-1}(\cos(\omega\Delta)-1) & 0 \\ 0 & \cos(\omega\Delta) & 0 & -\sin(\omega\Delta) & 0 \\ 0 & \omega^{-1}(\cos(\omega\Delta)-1) & 1 & \omega^{-1}\sin(\omega\Delta) & 0 \\ 0 & \sin(\omega\Delta) & 0 & \cos(\omega\Delta) & 0 \\ 0 & 0 & 0 & 0 & 1 \end{bmatrix},$$

$$\boldsymbol{G} = \begin{bmatrix} \Delta^2/2 & 0 & 0 \\ \Delta & 0 & 0 \\ 0 & \Delta^2/2 & 0 \\ 0 & \Delta & 0 \\ 0 & 0 & \Delta \end{bmatrix}$$

$\Delta = 1$ s and zero-mean noises $\boldsymbol{v}_{k-1} = [v_x, v_y, v_\omega]^{\mathrm{T}}$ with $\mathrm{cov}(v_x) = \mathrm{cov}(v_y) = 15\ \mathrm{m/s^2}$ and $\mathrm{cov}(v_\omega) = \pi/180$ rad/s.

The target birth process follows a Poisson point process with intensity $\gamma_k = \sum_{i=1}^{4} r_{k,i}\mathcal{N}(.;\boldsymbol{m}_i, \boldsymbol{Q})$, where $\boldsymbol{m}_1 = [-1500, 0, 250, 0, 0]^{\mathrm{T}}$, $\boldsymbol{m}_2 = [-250, 0, 1000, 0, 0]^{\mathrm{T}}$, $\boldsymbol{m}_3 = [250, 0, 750, 0, 0]^{\mathrm{T}}$, $\boldsymbol{m}_4 = [1000, 0, 1500, 0, 0]^{\mathrm{T}}$, $\boldsymbol{Q} = \mathrm{diag}([50, 50, 50, 50, \pi/30]^{\mathrm{T}})^2$ and $r_{k,1} = 0.02, r_{k,2} = 0.02, r_{k,3} = 0.03, r_{k,4} = 0.03$. If detected, the measurement is a noisy range and bearing vector given by

$$\boldsymbol{z}_k = \begin{bmatrix} \sqrt{p_{x,k}^2 + p_{y,k}^2} \\ \arctan\left(p_{x,k}/p_{y,k}\right) \end{bmatrix} + \boldsymbol{w}_k \tag{29}$$

where $\boldsymbol{w}_k \sim \mathcal{N}(.;\boldsymbol{0}, \boldsymbol{R}_k)$, with $\boldsymbol{R}_k = \mathrm{diag}([\sigma_r^2, \sigma_\theta^2]^{\mathrm{T}})$, $\sigma_r = 5$ m, $\sigma_\theta = \pi/180$ rad/s.

In the proposed SMC-PHD filter, 1000 particles per expected target are used and the total number of particles is hard-limited to be at least 600. We have noticed significant sample impoverishment caused by resampling,[49,50] although the number of particles used is larger than that in the last simulation. To combat this, we advocate the application of a simple yet powerful roughening strategy to rejuvenate the diversity of particles by adding Gaussian noise to each resampled particle. As suggested in Ref.[50], the roughening noise denoted as $\boldsymbol{\varrho}_k$ is designed with respect to the state process noise and is only carried out in position and velocity dimensions (excluding the turn-rate dimension that is nearly constant), i.e., $\boldsymbol{\varrho}_k = [\tau\boldsymbol{G}\boldsymbol{v}_{k-1}, 0]^{\mathrm{T}}$, where $\tau \in (0, 1]$ is a scaling parameter and we use $\tau = 1$ here. The roughening is simply carried out on resampled particle $\boldsymbol{x}_k^{(i)}$ by performing the following operation:

$$\boldsymbol{x}_k^{(i)} = \boldsymbol{x}_k^{(i)} + \boldsymbol{\varrho}_k \tag{30}$$

The true trajectories of targets are plotted in Fig. 5 where the colors distinguish different birth models and each trajectory starts from 'Δ' and ends at '$\square$'. The simulation parameters are: the target survival probability is $p_{\mathrm{S}} = 0.99$, and the target detection probability is $p_{\mathrm{D},k}(\boldsymbol{x}) = p_{\mathrm{D}} \times \mathcal{N}([p_{x,k}, p_{y,k}]^T; 0, 6000^2\boldsymbol{I}_2)/\mathcal{N}(0; 0, 6000^2\boldsymbol{I}_2)$. Clutter is uniformly distributed over the region with an average rate of r points per scan, i.e., $\kappa_k = r/2000/\pi$. In our simulation, we will adjust these two parameters: the clutter rate$r$ and the target detection probability p_D.

First, we set $r = 10$ and $p_{\mathrm{D}} = 0.95$. The sensor measurement in one trial is given in Fig. 6 in black circles where the true trajectories in the measurement space are given in blue lines.

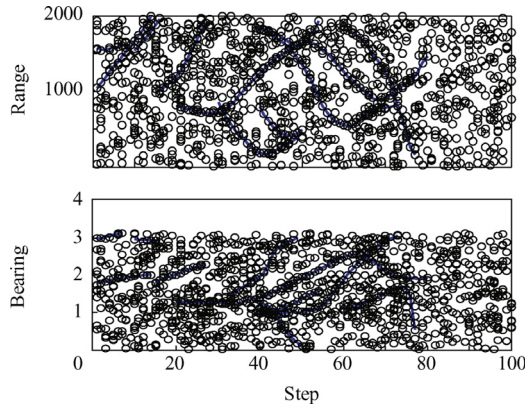

Fig. 6 Measurements of range and bearing when $r = 10$.

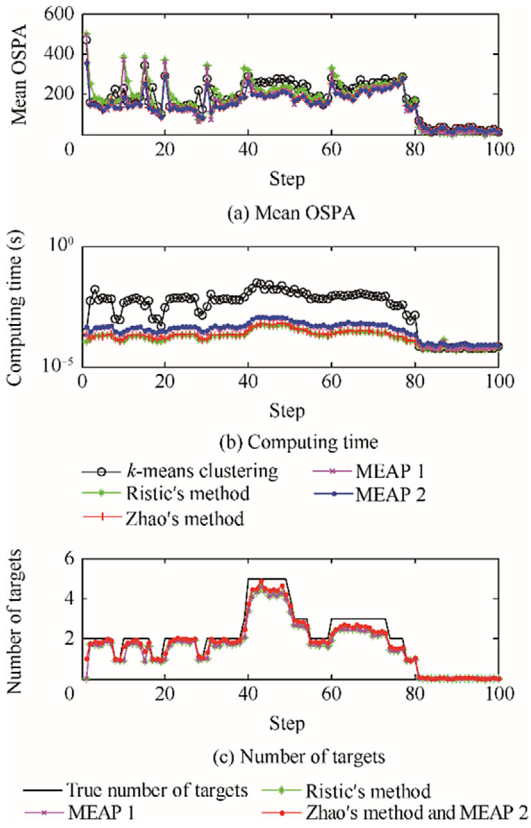

Fig. 7 Performance of different MEE methods when $r = 10$, $p_D = 0.95$.

The mean OSPA, computing time and estimated number of targets given by different methods are given separately in Fig. 7. Table 2 compares the improvement of different methods against that of the k-means (in terms of the percentage of reduction for OSPA and computing time). Compared with the result shown in the last simulation in Section 4.1, the advantage of the proposed MEAP estimators (as well as Zhao's method) is more significant with regard to estimation accuracy.

Secondly, we apply a wide range of clutter rate r from 0 to 50 and use a lower detection probability parameter $p_D = 0.9$. The improvement in terms of OSPA and computing time

Table 2 Performance improvement of different MEE methods vs. k-means clustering ($r = 10, p_D = 0.95$).

Metrics	Performance improvement (%)			
	Ristic's method	Zhao's method	MEAP 1	MEAP 2
OSPA	2.24	17.1	15.1	17.3
Time	96.8	96.5	93.8	93.0

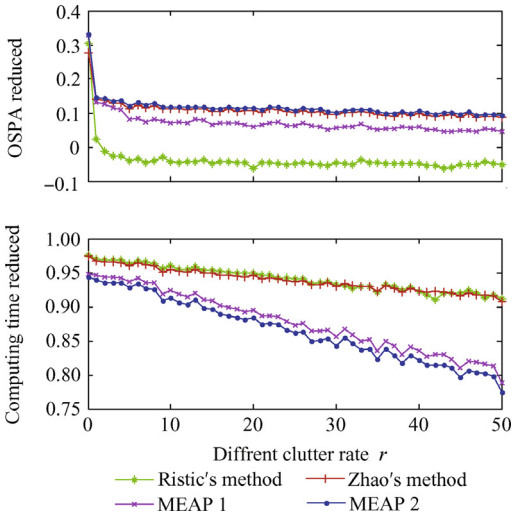

Fig. 8 Performance of different MEE methods for $r = 0 - 50$, $p_D = 0.9$.

achieved by the other methods, compared with the k-means for MEE for the same filter, are given in Fig. 8. The results are highly consistent with those of the last simulation with slight differences, which confirm that:

(1) Ristic & Zhao's methods, MEAP 1 and 2 have obtained much faster (greater than 80%) computing speed than the k-means clustering. The computing speed advantage, however, is not as large as was shown in the last simulation.
(2) Ristic's method has obtained lower estimation accuracy than others except for a very low clutter rate (but comparably not as bad as shown in the last simulation). Zhao's method and MEAP 2 obtained similar improvements (greater than 10% on average) on estimation accuracy than the k-means clustering regardless of whether SNR is low or high, which is somewhat different from the last simulation.
(3) MEAP 2 yielded the best accuracy performance overall, followed by Zhao's method.

To conclude the simulation results, the MEAP 2 outperformed the existing two primary classes of methods, consistently providing the best estimation accuracy and a much higher computing speed than clustering. If targets are close to one another, the correlation between them will highlight the unreliability of clustering methods while emphasizing the advantages of MEAP. When the targets are distant and the clutter rate is low, the MEAP is nearly the optimal EAP.

Please cite this article in press as: Li T et al. Multi-EAP: Extended EAP for multi-estimate extraction for SMC-PHD filter, *Chin J Aeronaut* (2017), http://dx.doi.org/10.1016/j.cja.2016.12.025

5. Conclusion

An easy-to-implement yet highly efficient estimator called MEAP is proposed for extracting the state-estimates of individual targets for the SMC-PHD filter. It formulates the MEE problem approximately as a family of single-target single-measurement sub-problems; each is solved by using a single-target EAP estimator. A fresh NNN principle is proposed to associate particles with each EAP estimator, reducing the correction between generated estimates. The proposed approach is free from iterative clustering computation and yields accurate estimation, resulting in highly independent state-estimates that best comply with reality. Simulations have demonstrated its superiority over state-of-the-art MEE methods in terms of both comparable computing speed and better estimation accuracy.

Two challenges remain open for more reliable and accurate MEE for the SMC-PHD filter, for which the proposed MEAP can be further extended to address. One is to better distinguish the clutter that is generated closely to real targets so as to circumvent false alarms. The other is to identify target misdetection and estimate the state of corresponding targets that are missed in detection. For these two intractable problems, the limited information of only a single frame is seemingly insufficient (though the PHD contains their information in theory, their signals are hard to identify). Instead one may have to resort to gathering information from multiple frames or even the extended information of targets. We emphasize that, MEE is not an isolated part for tracking but strongly coupled with track management. However, it would be particularly interesting to see how the MEAP estimator will perform on advanced SMC-PHD filters including the SMC-Cardinalized PHD filter and the multiple detection PHD filter in Ref.[37].

Acknowledgments

This work was partly supported by the Marie Skłodowska-Curie Individual Fellowship (No. 709267) under the European Union's Framework Programme for Research and Innovation Horizon 2020 and National Natural Science Foundation of China (No. 51475383).

References

1. Bar-Shalom Y, Li XR, Kirubarajan T. *Estimation with applications to tracking and navigation*. New York: John Wiley and Sons; 2001, p. 1–4.
2. Vo BN, Mallick M, Bar-shalom Y, Coraluppi S, Osborne R, Mahler R, Vo BT. *Multitarget tracking Wiley encyclopedia of electrical and electronics engineering*. New York: John Wiley and Sons; 2015, p. 1–15.
3. Li T, Fan H, Sun S. Particle filtering: theory, approach, and application for multi-target tracking. *Acta Autom Sinica* 2015;**41**(12):1981–2002 [Chinese].
4. Mahler R. *Advances in statistical multisource-multitarget information fusion*. Massachusetts: Artech House; 2014, p. 107–275.
5. Mahler R. Multi-target Bayes filtering via first-order multi-target moments. *IEEE Trans Aerosp Electron Syst* 2003;**39**(4):1152–78.
6. Williams JL. An efficient, variational approximation of the best fitting multi-Bernoulli filter. *IEEE Trans Signal Process* 2015;**63**(1):258–73.
7. García-Fernández ÁF, Vo BN. Derivation of the PHD and CPHD filters based on direct Kullback-Leibler divergence minimization. *IEEE Trans Signal Process* 2015;**63**(21):5812–20.
8. Vo BT, Vo BN, Cantoni A. The cardinality balanced multi-target multi-Bernoulli filter and its implementations. *IEEE Trans Signal Process* 2009;**57**(2):409–23.
9. Vo BT, Vo BN, Phung D. Labeled random finite sets and the Bayes multi-target tracking filter. *IEEE Trans Signal Process* 2014;**62**(24):6554–67.
10. Svensson L, Morelande M. Target tracking based on estimation of sets of trajectories. *Proceedings of the 17th international conference on information fusion*; 2014 July 8–10; Salamanca, Spain. Piscataway (NJ): IEEE Press; 2014. p. 1–8.
11. Clark D, Bell J. Multi-target state estimation and track continuity for the particle PHD filter. *IEEE Trans Aerosp Electron Syst* 2007;**43**(4):1441–53.
12. Vo BN, Singh S, Doucet A. Sequential Monte Carlo methods for multi-target filtering with random finite sets. *IEEE Trans Aerosp Electron Syst* 2005;**41**(4):1224–45.
13. Dunne D, Ratnasingham T, Lang T, Kirubarajan T. SMC-PHD based multi-target tracking with reduced peak extraction. In: Drummond OE, Teichgraeber RD, editors. *SPIE proceedings of signal and data processing of small targets*; 2009 August 2; San Diego, CA; Washington, D.C.: SPIE Press; 2009. p. 74450F-1-12.
14. Liu W, Han C, Lian F, Zhu H. Multitarget state extraction for the PHD filter using MCMC approach. *IEEE Trans Aerosp Electron Syst* 2010;**46**(2):864–83.
15. Tobias M, Lanterman AD. Techniques for birth-particle placement in the probability hypothesis density particle filter applied to passive radar. *IET Radar Sonar Navig* 2008;**2**(5):351–65.
16. Tang X, Wei P. Multi-target state extraction for the particle probability hypothesis density filter. *IET Radar Sonar Navig* 2011;**5**(8):877–83.
17. Xu B, Xu H, Zhu J. Ant clustering PHD filter for multiple-target tracking. *Appl Soft Comput* 2011;**11**(1):1074–86.
18. Zhao L, Ma P, Su X. An improved peak extraction algorithm for probability hypothesis density particle filter. *Adv Sci Lett* 2012;**6**(1):88–95.
19. Lin L, Xu H, Sheng W, An W. Multi-target state-estimation technique for the particle probability hypothesis density filter. *Sci China E: Inform Sci* 2012;**55**(10):2318–28.
20. Si W, Wang L, Qu Z. A measurement-driven adaptive probability hypothesis density filter for multitarget tracking. *Chin J Aeronaut* 2015;**28**(6):1689–98.
21. Baum M, Willett P, Hanebeck UD. MMOSPA-based track extraction in the PHD filter - a justification for k-means clustering. *Proceedings of IEEE 53rd annual conference on decision and control*; 2014 December 15–7; Los Angeles, CA. Piscataway (NJ): IEEE Press; 2014. p. 1816–21.
22. Zhao L, Ma P, Su X, Zhang H. A new multi-target state estimation algorithm for PHD particle filter. *Proceedings of the 13th international conference on information fusion*; 2010 July 26–29; Edinburgh, UK. Piscataway (NJ): IEEE Press; 2014. p. 1–8.
23. Ristic B, Clark D, Vo BN. Improved SMC implementation of the PHD Filter*Proceedings of the 13th international conference on information fusion; 2010 July 26–29; Edinburgh, UK*. Piscataway (NJ): IEEE Press; 2010. p. 1–8.
24. Wood TM, Clark D, Ristic B. Efficient resampling and basic track continuity for the SMC-PHD filter. *Proceedings of cognitive systems with interactive sensors*; 2010 November 22; Crawley, UK. London: IET Press; 2010. p. 1–6.
25. Schikora M, Koch W, Streit R, Cremers D. Sequential Monte Carlo method for multi-target tracking with the intensity filter. In: Georgieva P, Mihaylova L, Jain LC, editors. *Advances in intelligent signal processing and data mining: theory and applications*. Berlin: Springer; 2012. p. 55–87.
26. Degen D, Govaers F, Koch W. Emitter localization under multipath propagation using SMC-Intensity filter. *Proceedings of*

the 16th international conference on information fusion; 2013 July 10–2; Istanbul, Turkey. Piscataway (NJ): IEEE Press; 2013. p. 1–8.
27. Li Y, Xiao H, Fan H, Fu Q. Free-clustering optimal particle PHD filter for multi-target tracking. *J Cent South Univ* 2014;**21**:2673–83.
28. Bozdogan AO, Efe M, Streit R. Reduced palm intensity for track extraction*Proceedings of the 16th international conference on information fusion; 2013 July 10–2; Istanbul, Turkey*. Piscataway (NJ): IEEE Press; 2013. p. 1243–50.
29. Crouse DF, Willett P, Bar-Shalom Y. Developing a real-time track display that operators do not hate. *IEEE Trans Signal Process* 2011;**59**(7):3441–7.
30. Lin L, Bar-Shalom Y, Kirubajan T. Track labeling and PHD filter for multitarget tracking. *IEEE Trans Aerosp Electron Syst* 2006;**42**(3):778–95.
31. Boers Y, Sviestins E, Driessen H. Mixed labelling in multitarget particle filtering. *IEEE Trans Aerosp Electron Syst* 2010;**46**(2):792–802.
32. García-Ferna´ ndez AF, Vo BN, Vo BT. MCMC-based posterior independence approximation for RFS multitarget particle filters. *Proceedings of the 17th international conference on information fusion*; 2014 July 8–10; Salamanca, Spain. Piscataway (NJ): IEEE Press; 2014. p. 1–8.
33. Caron F, Moral PD, Doucet A, Pace M. On the conditional distributions of spatial point processes. *Adv Appl Probab* 2011;**43**(2):301–7.
34. Singh SS, Vo BN, Baddeley A, Zuyev S. Filters for spatial point processes. *SIAM J Control Optim* 2009;**48**(4):2275–95.
35. Ristic B, Beard B, Fantacci C. An overview of particle methods for random finite set models. *Inform Fus* 2016;**31**:110–26.
36. Li T, Sun S, Bolic M, Corchado JM. Algorithm design for parallel implementation of the SMC-PHD filter. *Signal Process* 2016;**119**:115–27.
37. Tang X, Chen X, McDonald M, Mahler R, Tharmarasa R, Kirubarajan T. A multiple-detection probability hypothesis density filter. *IEEE Trans Signal Process* 2015;**63**(8):2007–19.
38. Streit R, Degen C, Koch W. The pointillist family of multitarget tracking filters; 2015. Available from: arXiv:1505.08000.
39. Li T, Bolić M, Djurić P. Resampling methods for particle filtering: classification, implementation, and strategies. *IEEE Signal Process Mag* 2015;**32**(3):70–86.
40. Kay SM. *Fundamentals of statistical signal processing: estimation theory*. Englewood Cliffs (NJ): Prentice Hall; 1993, p. 344–350.
41. Degen C, Govaers F, Koch W. Track maintenance using the SMC-intensity filter. *Proceedings of 2012 workshop on sensor data fusion: trends, solutions, applications*; 2012 September 4–6; Bonn, Germany. Piscataway (NJ): IEEE Press; 2012. p. 7–12.
42. Yazdian-Dehkordi M, Azimifar Z. An improvement on GM-PHD Filter for target tracking in presence of subsequent miss-detection. *Proceedings of the 23rd Iranian conference on electrical engineering*; 2015 May 10–4; Tehran, Iran. Piscataway (NJ): IEEE Press; 2015. p. 765–9.
43. Yang J, Ji H. A novel track maintenance algorithm for PHD/CPHD filter. *Signal Process* 2012;**92**(10):2371–80.
44. Li T, Sun S, Corchado JM, SiyauMF. A particle dyeing approach for track continuity for the SMC-PHD filter. *Proceedings of the 17th international conference on information fusion*; 2014 July 8–10; Salamanca, Spain. Piscataway (NJ): IEEE Press; 2014. p. 1–8.
45. Williams JL. Hybrid Poisson and multi-Bernoulli filters. *Proceedings of the 15th international conference on information fusion*; 2012 July 9–12; Singapore. Piscataway (NJ): IEEE Press; 2012. p. 1103–10.
46. Pierre DM, Houssineau J. Particle association measures and multiple target tracking. In: Peters GW, Matsui T, editors. *Theoretical aspects of spatial-temporal modeling*. Tokyo (Japan): Springer; 2015. p. 1–30.
47. Ouyang C, Ji H, Guo Z. Extensions of the SMC-PHD filters for jump Markov systems. *Signal Process* 2012;**92**(6):1422–30.
48. Schuhmacher D, Vo BT, Vo BN. A consistent metric for performance evaluation in multi-object filtering. *IEEE Trans Signal Process* 2008;**56**(8):3447–57.
49. Li T, Villarrubia G, Sun S, Corchado JM, Bajo J. Resampling methods for particle filtering: identical distribution, a new method and comparable study. *Front Inform Technol Electron Eng* 2015;**16**(11):969–84.
50. Li T, Sattar TP, Sun S, Han Q. Roughening methods to prevent sample impoverishment in the particle PHD filter. *Proceedings of the 16th international conference on information fusion*; 2013 July 9–12; Istanbul, Turkey. Piscataway (NJ): IEEE Press; 2013. p. 17–22.

Please cite this article in press as: Li T et al. Multi-EAP: Extended EAP for multi-estimate extraction for SMC-PHD filter, *Chin J Aeronaut* (2017), http://dx.doi.org/10.1016/j.cja.2016.12.025